

Increasing the Electrochemical Activity of Basal Plane Sites in Porous 3D Edge Rich MoS₂ Thin Films for the Hydrogen Evolution Reaction

Sha Li¹, Si Zhou¹, Xiaochen Wang¹, Peng Tang¹, Mauro Pasta^{1}, Jamie H. Warner^{1*}*

¹Department of Materials, University of Oxford, 16 Parks Road, OX1 3PH, UK

Email: jamie.warner@materials.ox.ac.uk; mauro.pasta@materials.ox.ac.uk;

Abstract

Molybdenum disulfide (MoS₂) has been extensively utilized as an electrocatalyst for the hydrogen evolution reaction (HER) with edges as the primary active catalytic sites. Previous work on edge-rich MoS₂ nanoplatelet 3D porous films (3D-ER-MoS₂) shows they are promising catalysts, yet have basal planes that are inactive. Here we demonstrate how hydrogen annealing and oxygen plasma etching of 3D-ER-MoS₂ generates defects and increases active site density within the basal plane, leading to dramatic improvements in HER catalytic activity. We also explore the critical processing parameters for electrocatalytic enhancement. Significantly enriched edge density was revealed for both routes. O₂ plasma treatment was more effective in increasing the number of edges by creating micro-cracks and local surface damage on the basal planes as well as structuring saw-toothed edges; H₂ etching mainly introduced irregular shaped basal surface nanopores and strips. By controlling processing parameters, optimum surface area/active sites density enhancement can be achieved, together with the robust 3D porous architecture and superaerophobic surface. The defect-rich MoS₂ catalysts exhibit excellent HER activity: 700 °C – H₂ – MoS₂ shows Tafel slope of 94 mV/dec and

low onset overpotential of 193 mV; 15 mins – O₂ – MoS₂ performs amongst the best with excellent exchange current density of 57 $\mu\text{A}/\text{cm}_{\text{geo}}^{-2}$. Our defect engineered 3D-ER MoS₂ exhibits j_{geo} ($\eta=0.5$ mV) of 6-fold and 38-fold compared to monolayer MoS₂ subject to similar process, for O₂ plasma and H₂ etching approaches respectively. Our study demonstrates an effective way to realize high performance Pt-free electrocatalysts for hydrogen generation by dual enhancement via edge enrichment and basal surface activation.

Keywords: Surface area enhancement; Defect engineering; Edge enrichment; MoS₂ vertically standing nanoplatelets; Hydrogen evolution reaction (HER);

Introduction

Water electrolysis is a clean approach to produce hydrogen, which holds promise for a more sustainable energy future for society.^{1–5} Electrocatalysts are needed at the electrode to lower the overpotential and consequently increase the efficiency of hydrogen production.⁶ The commercial Pt catalysts exhibit excellent activity but their widespread use is limited by scarcity and high cost.⁷ In order to advance the long term future of hydrogen energy, non-noble metal alternatives must be explored in place of Pt.⁸ In the past years, MoS₂ has been considered as a promising alternative candidate to Pt metals because of its low price, abundance and high activity towards HER.^{9,10}

Both theoretical and experimental studies confirmed that the edges of MoS₂ are catalytic active due to unsaturated sulfur atoms at the edge sites with dangling bonds.^{10–13} Moreover, 1T phase of MoS₂ produced by solution-phase lithium intercalation has been effective in enhancing the electrocatalytic performance further by modifying the electronic structure of the MoS₂.^{14,15} But such 1T polymorphs are challenging to produce by non-solution based methods such as in the case of chemical vapor deposition (CVD) method, which is promising for wafer scale, high quality and clean production of the controllable 3D porous network. For CVD grown MoS₂ materials, the focus has been on how to enrich the edges to increase HER activity. Efforts have been put into maximizing the edge density of

MoS₂ catalysts by shape control, support variation for highly dispersed catalyst particles and nanostructuring.^{1,10,16–26} Kong et al. has demonstrated vertically aligned atomic MoS₂ layers with maximized edge exposure for enhanced HER.²⁷ Our previous study demonstrated the synthesis of vertically standing nanoplatelet films for improved HER application with enriched edge density by a one-step CVD approach.²⁸ Apart from high edge density, this morphology also facilitates high surface area (real to geometric area ratio of as high as 300) due to the 3D porous structure and thus possesses a huge area of basal planes inside such a structural configuration.^{29,30} The demonstrated CVD synthesis route for superaerophobic surface holds superiority to previous work, where precise tuning of desirable defects, structure and surface area encountered difficulties due to the hard-to-control hydrothermal synthesis approach.^{54,55}

Although the edges are enriched in porous 3D MoS₂ branched films, the vast amount of catalytic inactive basal planes left unutilized strongly impedes the optimization of HER performance of the MoS₂ catalysts.^{31,32} Also, there has been lack of correlation of structural modification with HER optimization due to the difficulty in identifying detailed HER active structure.²⁴ Defect treatment can be used to introduce additional edges by generating micro cracks and voids to the inert MoS₂ basal planes as well as pre-existing edges in order to increase the number of edge sites and consequently improve the catalytic activity.^{10,24,33–38} A previous study has found that Mo-O doping can assist the photoluminescence of monolayer MoS₂.³⁹ O₂ annealing of thick MoS₂ has been reported to be an effective way to introduce randomly oriented and controllable triangular etched shapes, forming pits with uniform etching angles.^{24,38,40–42} Tuning of the etching process parameters resulted various ordered structures.⁴³

Research on etching of graphene has demonstrated that Ar/H₂ gas mixture can be used to etch the graphene sample by forming hexagonal holes with zigzag edge structures, and a similar study has also been carried out on WS₂ materials.^{44,45} HER activity enhancement by activation of the basal

plane surfaces via such defect engineering has been realized on monolayer MoS₂, but the physical area of the electrode has been underutilized by the limited number of edges resulted from merely one atomic layer of active material deposited onto the surface.²⁴

Here, we demonstrate a method for combining the maximized usage of electrode area and activation of catalytically inert basal surfaces by gas phase etching of CVD-grown 3D edge rich MoS₂ vertically standing nanoplatelet films. We study two different approaches for post synthesis treatments: 1. oxygen (O₂) plasma exposure at room temperature, and 2. High temperature hydrogen (H₂) annealing to enhance the edge density of the primary catalyst by adding new micro cracks and pores. Both O₂ plasma exposure and H₂ etching significantly improved the HER activity of pristine MoS₂, with H₂ etching being more effective than O₂ plasma. Controllable microstructure and morphology of defect modulation can be achieved by tuning the parameters of post-growth treatments, such as annealing temperature and plasma exposure time. Furthermore, the quantitative correlation between surface area enhancement and catalytic improvement is explored. Such deliberate processes provide governing guidelines behind the electrochemical change and open up new way for noble metal free catalyst design and optimization.

Results and Discussion

Figure 1 depicts the defect engineering route utilizing O₂ plasma and H₂ etching approaches in order to introduce vacancies, cracks and pores that provide additional edges into the pristine MoS₂ catalyst system and consequently enhance the HER activity.

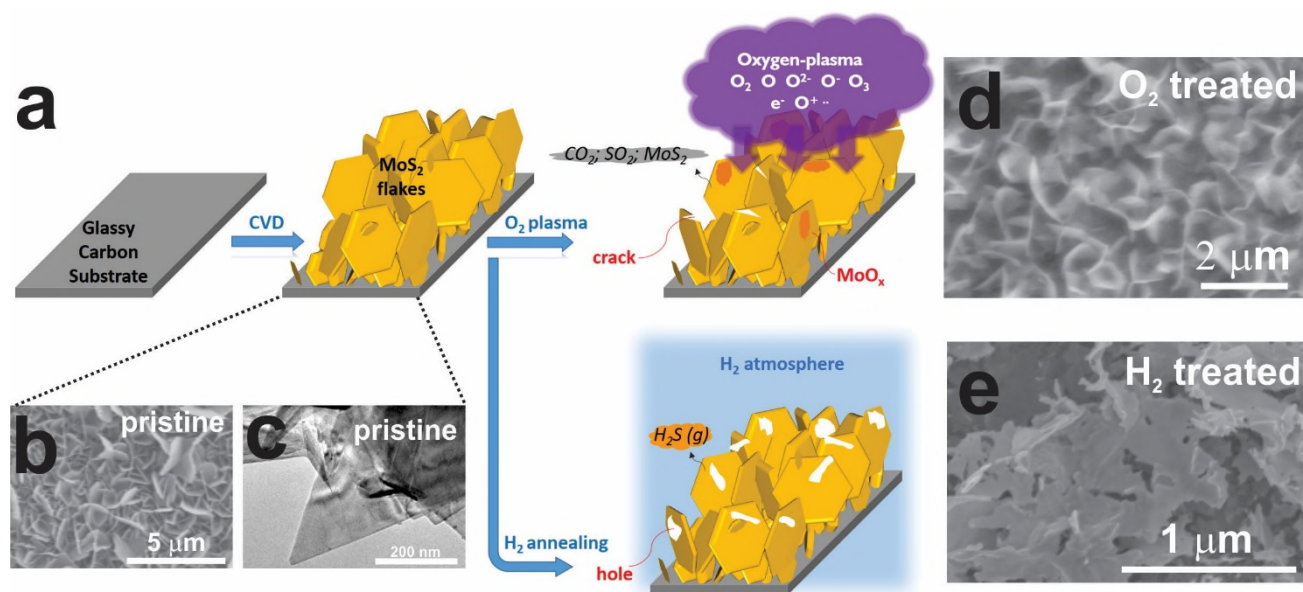


Figure 1. (a) Schematic of gas phase treatments of CVD grown MoS₂ thin film catalysts by either utilizing O₂ plasma or H₂ etching approaches. SEM images showing the morphology of (b) pristine (TEM image in c showing a typical triangular domain), (d) O₂ plasma etched and (e) H₂ etched CVD MoS₂ thin film.

As reported in our previous study, the pristine MoS₂ was synthesized by one step CVD method using MoO₃ and S powder precursor grown at 866 °C for 1h, yielding vertically standing nanoplatelet morphology, 3D porous architecture and superaerophobic surface. This catalyst film is grown directly onto glassy carbon (GC) in order to be incorporated into the electrochemical testing setup as a working electrode to investigate the catalytic properties of as-prepared materials, without introducing any additional transfer processes. Then, the CVD as-synthesized MoS₂ thin films on GC are subject to O₂ plasma exposure to create surface cracks and oxide phases via bombardment and reaction of the surface materials with O₂ plasma; and H₂ etching to generate irregular shaped holes onto the basal surfaces by chemical reaction etching. O₂ plasma was carried out at pressure of 0.8~1 mPa for 0, 15 and 30 mins in order to etch the materials and create defects such as pores and cracks. SEM and (in-situ) TEM were used to investigate the effect of O₂ plasma on morphological and microstructural change. SEM images as in Fig. S1 demonstrate that there's no obvious microscopic changes before and after O₂ plasma treatment – the edge exposed vertical alignment of the flakes are

well preserved. Based on our TEM analysis, the plasma mainly introduces three types of defects to the pristine domains: (1) edge-roughening by serration/steps on the edge sites, (2) micro cracks and (3) local damage on the basal surfaces; all accompanying material loss. MoS₂ flakes before plasma treatment depicted in Fig. 2a-d possess clean and smooth edges at both nanoscale and atomic scale.

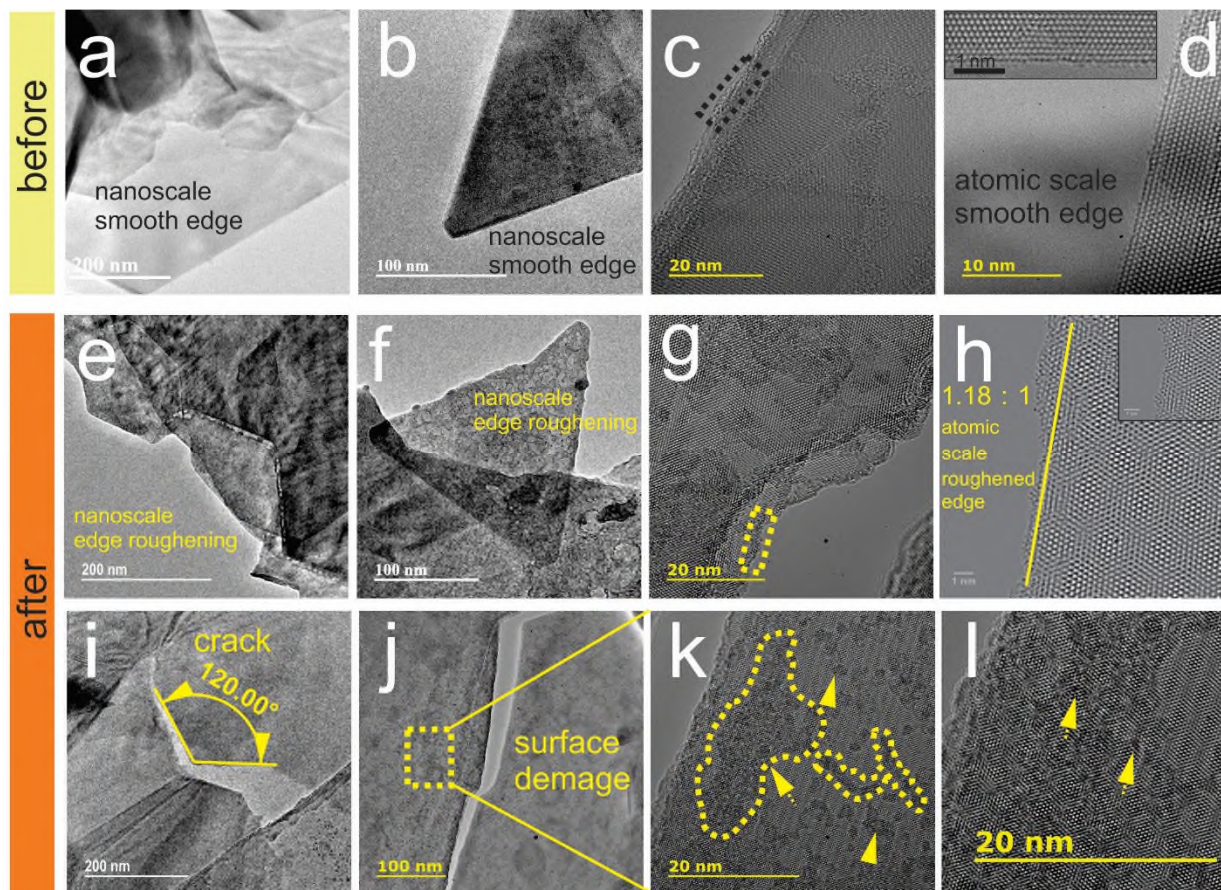


Figure 2. Effect of O₂ plasma treatment on morphology and microstructure of MoS₂ nanoplatelets. TEM images of MoS₂ flakes before O₂ plasma treatment exhibiting clean and smooth edges at (a and b) nanoscale and (c and d) atomic scale. TEM visualization of three types of defects induced by 15 mins O₂ plasma exposure: roughened edges at (e and f) nanoscale and (g and h) atomic scale; (i) micro cracks and (j-l) basal surface damages at different magnifications.

In order to understand the microstructure configuration of the O₂ plasma induced defects in the catalyst, TEM imaging was undertaken by exposing MoS₂ on a lacey carbon grid to O₂ plasma for 2 min and monitor any structure change of the same area before and after plasma etching. TEM images

in Fig. 2e and f show the nanoscale edge structure of the MoS₂ after treatment. Compared with pre-treated sample, steps/serrations have been introduced to the edges, resulting in an increase in the number of edge sites for catalytic reaction, which will be discussed in detail later. HRTEM images in Fig. 2g and h verify the edges are roughened at atomic level. Micro cracks on the basal planes of MoS₂ can be seen from Fig. 2i, with 120° orientation, which can attribute to the crystallographic symmetry of the MoS₂ material. Fig. 2j shows the surface damage that resulted from the plasma etching process, resulting in nanopores on the basal surfaces, which helps to expose more edges on the otherwise catalytic inactive basal sites. The detailed structure of basal surface damage can be observed from the yellow circle in Fig. 2k and 2l, showing that across the basal surface of the few layered flakes there are defects across the surface that arises from the O₂ plasma etching of the MoS₂ surface. The combination of the aforementioned three types of defects demonstrates that the O₂ plasma treatment is a powerful method to create additional edge sites by etching the platelets at both nanometer and atomic level, which aligns very well with the surface area evaluation in Fig. 4 and is thought to be beneficial for HER activity by increasing the edge density.

Raman spectroscopy was conducted to examine the chemical composition of the O₂-etched sample. The Raman spectrum shown in Fig. 3a confirms the CVD grown material is MoS₂, with the two characteristic peaks revealed, corresponding to the two vibrational modes of MoS₂: in-plane vibration of molybdenum and sulfur atoms E_{2g}¹ and out-of-plane vibration of sulfur atoms A_{1g}, which is consistent with literature.^{19,25}

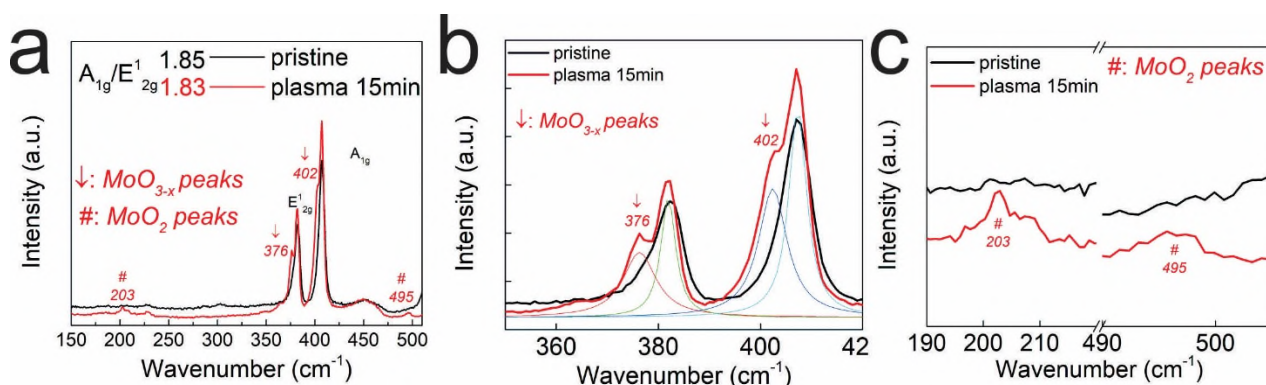


Figure 3. Chemical composition influenced by O₂ plasma treatment. (a) Raman spectra of CVD as prepared and 15 mins O₂ plasma treated MoS₂ catalysts. Inset: two characteristic Raman vibration modes in MoS₂: in-plane vibration of molybdenum and sulfur atoms E_{2g}¹ and out-of-plane vibration of sulfur atoms A_{1g}; information on peak intensity ratio of A_{1g}/E_{2g}¹ of samples before and after O₂ plasma treatment (1.83 and 1.85, respectively); oxidation induced peaks. Characteristic peaks indicating (b) MoO_{3-x} and (c) MoO₂ phases, respectively.

The comparable peak intensity ratio A_{1g}/E_{2g}¹ before and after O₂ plasma confirms that the vertical alignment of the thin film has been maintained after being treated with O₂ plasma. It's also revealed that O₂ plasma treatment does involve a small amount of oxidation of MoS₂ evidenced by the oxides peaks as indicated for (b) MoO_{3-x} and (c) MoO₂ phases. The effect of oxide phase on HER activity will be discussed later on.

The real surface area evaluation and electrochemical testing were carried out to investigate the efficiency and effectiveness of O₂ plasma on the surface area and HER activity enhancement (Fig. 4).

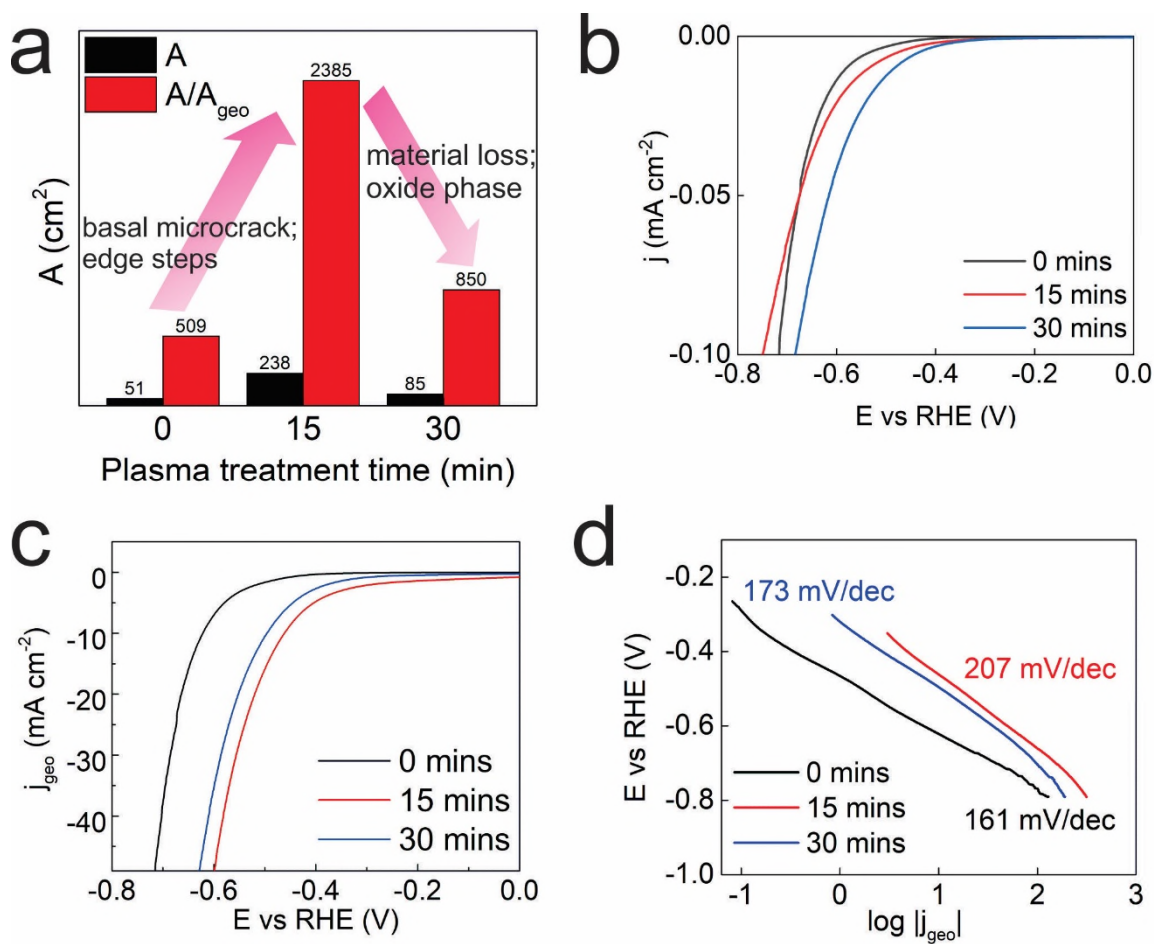


Figure 4. Effect of O_2 plasma etching on surface area and electrochemical activity of 3D-ER MoS_2 . (a) Surface area evaluation as a function of O_2 plasma etching time (A_{geo} : geometric area of the catalyst; A : real surface area of the catalyst). Cathodic polarization curves at scan rate of 1 mV/s normalized by (b) geometric area and (c) real surface area. (d) Tafel plots of O_2 plasma treated samples under different exposure periods.

Compared to the as-grown sample, O_2 plasma etching exhibits excellent potential in enhancing the surface area/edge density (Fig. 4a: 5-fold of the untreated sample at 15 mins exposure time; 2-fold at 30 mins exposure time). The lower surface area enhancement for the 30 mins treatment time results from the materials loss at prolonged plasma exposure periods. Real surface area normalized current density j is a fairly good indicator of the intrinsic activity (i.e. turn over frequency) of the material. It can be seen from Fig. 4b that the onset overpotential of plasma treated sample remains almost unchanged compared to the untreated one, indicating the type of the catalytic active sites hasn't changed – Mo edges in MoS_2 act as catalytic sites for HER. There is a certain degree of improvement

in terms of the cathodic current density when the plasma exposure time increases. It can attribute to the lowered crystallographic symmetry and increased lattice distortion of MoS₂ under oxygen plasma treatment, which are beneficial to the HER electrocatalytic activity.^{24,26}

When it comes to the device oriented activity (normalized by the geometric area of the electrode), there is obvious improvement from the oxygen plasma treatment, which is consistent with the inherent activity enhancement as discussed above. It is also seen that j_{geo} reaches a maximum at 15 mins exposure time and longer exposure leads to smaller improvement, following the trend of the real surface area measurement in Fig 4a, although the intrinsic activity increases linearly with extended plasma exposure time.

When discussing the aforementioned trend of overall catalytic activity, the following four factors need to be taken into consideration:

- 1) Oxygen plasma induces defects, contributing to inherent activity improvement;
- 2) Oxygen plasma treatment increases edge density in the form of serrated edges, microcracks and surface nanopores;
- 3) Catalyst material loss occurs due to the destructive plasma etching;
- 4) Chemical change of catalytically active and semiconducting sulfide to catalytically unfavorable but conductive oxide phases (MoO₂ and MoO_{3-x}).

After 15 mins of oxygen plasma, the activity per edge site is improved due to defects as discussed in Fig. 4b; the number of edges is significantly increased from surface cracks, nanopores and serrated edges, as evidenced from the surface area measurement in Fig. 4a. The two factors combine to improve the overall HER activity for 15 mins exposure time. When the oxygen plasma exposure time is increased to 30 mins, the activity per site is still further increased as in Fig. 4b, but the edge density/surface area enhancement is limited by the loss of material. Therefore a lower surface area is seen for 30 mins compared to 15 mins (Fig. 4a). Following the trend of the surface area measurement,

the overall electrochemical activity of the 30-min treated sample also exhibits smaller improvement than for 15-min, which indicates the increased activity per site can't be compensated by the active materials loss.

Next we discuss the impact of the oxide phase in this materials system for HER. There has been suggestions that MoO_3 is soluble in acid and will not play a role in HER in acid media.²⁴ This explanation doesn't necessarily apply to our system because we can't be assured the oxides have been formed at acid accessible locations, given the 3D porous structure of the material. As revealed by Raman spectroscopy, molybdenum oxide phases were formed in the catalyst system which possesses better conductivity than MoS_2 and is beneficial to circumvent the conductivity limitation from the semi-conductive nature of MoS_2 . But from the electrochemical impedance spectroscopy analysis in Fig. S2, it's obvious that the entirety of the measured series resistance doesn't appear to differ significantly across samples with/without plasma exposure (range: 20 ~ 50 Ω/cm^2). This ensures that at such oxygen plasma exposure levels, the effect of as-generated oxides on lowering the Ohmic resistance of the catalytic system is negligible, or less significant than decreasing total amount of catalytic active materials (MoS_2).

This shows that the inherent activity and real surface area are enlarged by O_2 plasma treatment. Consequently, the total electrode activity is improved. Exchange current density is significantly enhanced by 18-fold (as seen in Table 1). It indicates the rate of reaction at the reversible potential (when the over-potential is zero by definition) and was obtained from Tafel plots by extrapolation method. The Tafel slope is characteristic of the electrocatalyst surface determining the HER rate-limiting step and is used to indicate the catalytic properties and HER mechanisms. In the acid media, HER may occur through either Volmer ($\text{H}^+ + \text{e}^- \rightarrow \text{H}_{\text{ad}}$, 120 mV/dec) – Tafel ($\text{H}_{\text{ad}} + \text{H}_{\text{ad}} \rightarrow \text{H}_2$, 30 mV/dec) or Volmer – Heyrovsky ($\text{H}^+ + \text{e}^- + \text{H}_{\text{ad}} \rightarrow \text{H}_2$, 40 mV/dec) mechanism.⁴⁷ The rate-limiting step of plasma etched samples remained unchanged compared to the untreated sample and indicates

a Volmer reaction. The increased Tafel slope value of the oxygen plasma treated samples as seen from Fig. 4d indicates a higher overpotential is required in order to enhance the same amount of current density. By comparison of overall HER performance under different treatment times, 15 mins is the optimum condition in order to improve hydrogen production, real surface area, conductivity and Tafel slope as well as exchange current density.

An alternative gas phase etching approach is annealing in H_2 gas flow, which is likely to strip sulfur from MoS_2 and leave S vacancy defects, and under high temperatures may lead to Mo removal as well. The CVD grown MoS_2 nanoplatelets were etched under Ar/H_2 gas atmosphere at 600, 700 and 800 °C. SEM measurements of samples annealed at different temperatures are summarized in Fig. 5b-d.

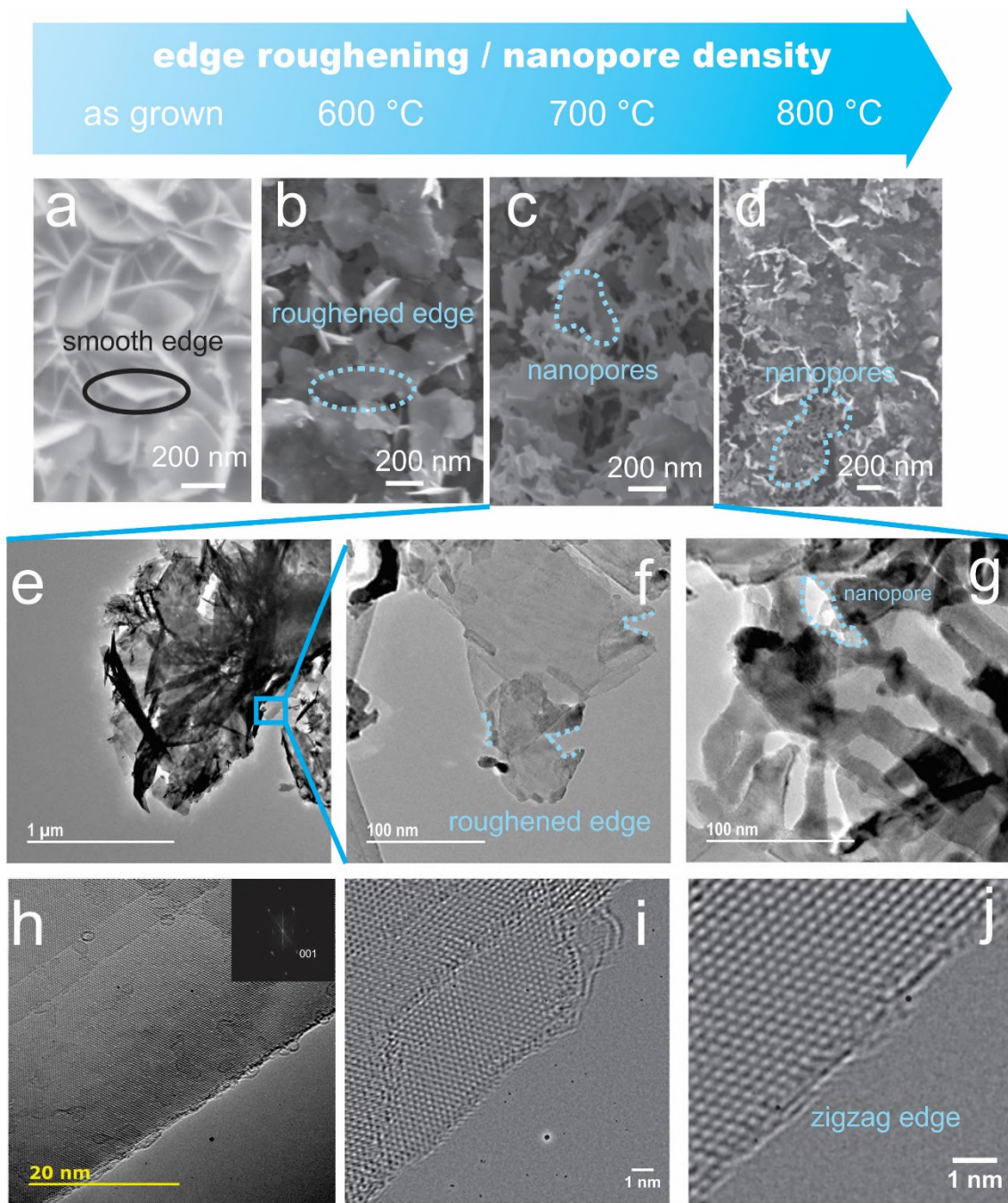


Figure 5. Structural investigation of the H₂ etched sample. (a-d) SEM images of the MoS₂ catalysts as-grown and etched by H₂ at 600, 700 and 800 °C, respectively. (e-g) TEM images of 700 °C H₂ annealed MoS₂ flakes, depicting roughened edges and formation of nanopores and nanoribbons. (h-j) HRTEM images of 700 °C H₂ annealed MoS₂ flakes demonstrating atomic scale edge configuration, inset: FFT of Fig. 5h.

The as-grown sample (Fig. 5a) consists of perfectly smooth vertically standing nanoplatelets, but when annealed in H₂ at 600 °C, serrated features start to emerge at the edges of the nanoplatelets. With temperature elevated to 700 °C, along with etched and serrated edges, pores are found to be created on the basal surfaces. As the temperature is further increased to 800 °C, more material has been etched away and the whole thin film becomes significantly ragged, with some spots of the substrate being exposed. The higher the annealing temperature, the larger the density of the holes are created on the basal surfaces, indicating loss of both S and Mo atoms. TEM imaging was used to study H₂ etching induced microstructure changes. Fig. 5e-g shows that H₂ annealing promotes the formation of a large number of irregular shaped and oriented nanopores and nanoribbons, which leads to an irregular hollow and serrated configuration across the thin film catalyst surface. HRTEM images of the same H₂ annealed sample are shown in Fig. 5h-j. As opposed to O₂ plasma etching which increases the edge density by creating atomic roughened edge configuration, the edges of the H₂ annealed platelets retain their clean and smooth form as in the pristine one with zigzag direction as evidenced in Fig. 5h inset. The edge density enhancement mainly arises from what has been discussed – formation of networked nanopores and nanoribbons.

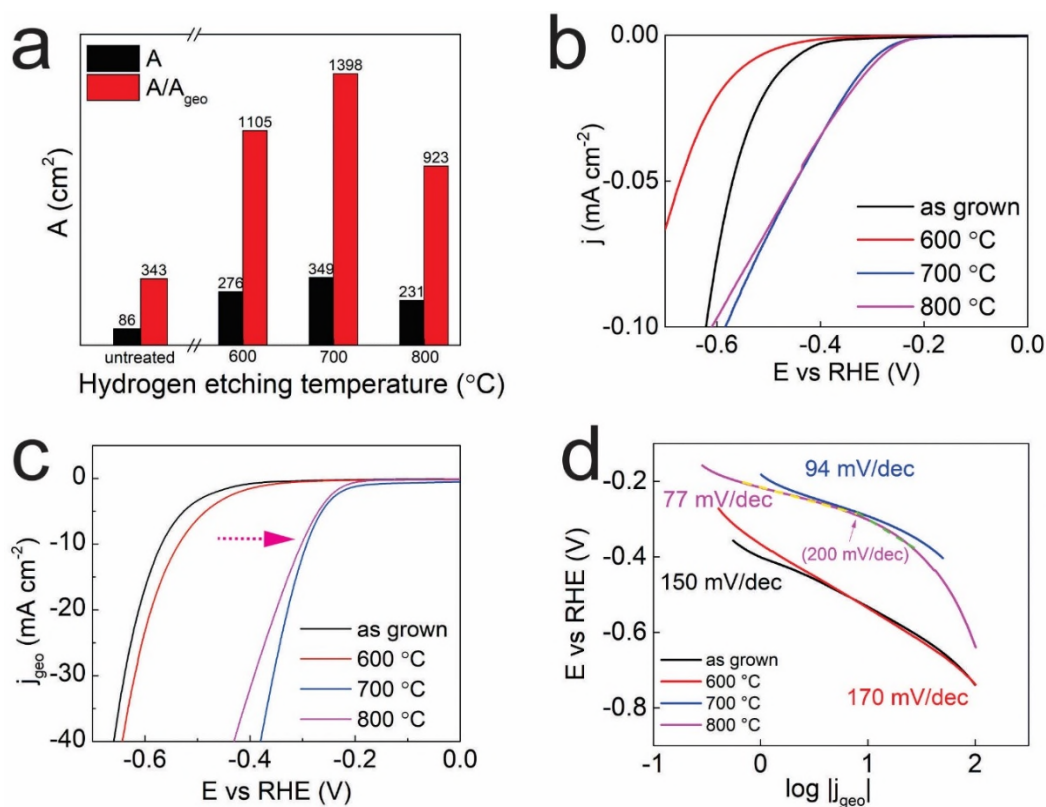


Figure 6. Chemical composition and HER performance of the H₂ annealed 3D-ER MoS₂. (a) Surface area evaluation of H₂ etching process as a function of H₂ etching temperatures (A_{geo} : geometric area of the catalyst; A : real surface area of the catalyst). Cathodic polarization curves at scan rate of 1 mV/s at different H₂ annealing temperatures normalized by (b) geometric area and (c) real surface area. (d) Tafel plots of the H₂ etched samples under different annealing temperatures.

Raman spectroscopy was used to inspect possible chemical compositional changes introduced by H₂ annealing. As seen in Fig. S3, the Raman spectrum of the H₂ etched sample at 700 °C exhibits the two characteristic peaks of MoS₂. The intensity ratio of A_{1g}/E_{2g}^1 matches well with the untreated sample, indicating the vertical alignment of the nanoplatelet is well maintained after high temperature reducing atmosphere H₂ etching. At the same time, blue shift for both peaks is observed. The E_{2g}^1 vibration is studied to be affected solely by built-in strain; while A_{1g} vibrational mode is an indicator of the doping level.⁴⁸ The blue shift of E_{2g}^1 peak can be attributed to the strain released when annealed at high temperature (700 °C) for 2h.

Surface area changes in Fig. 6a reveal that H₂ annealing is effective in enhancing surface area of the materials. As annealing temperature increases, the surface area enhancement first increases, reaches a maximum at 700 °C (4-fold of the untreated sample, Fig 6a) and decreases at 800 °C. A temperature lower than 700 °C may not be sufficient to effectively etch MoS₂ and expose as many new surfaces as 700 °C; whereas 800 °C is high enough that material loss and decomposition start to play dominant roles and lead to lowered surface area enhancement.

The polarization curves normalized by real surface area as in Fig. 6b reveal the intrinsic activity per active site in the material. The 600 °C sample is found to start evolving hydrogen at similar overpotential as the untreated sample, indicating that at this point the type of active site hasn't changed – MoS₂ edges are dominant active sites. But the current density of 600 °C is smaller than the pristine one, due to the elimination of defects that attribute to inherent catalytic activity.^{47,49-51} Samples annealed at 700 and 800 °C exhibit similar onset overpotential and both are much smaller than the untreated sample. One possible reason to this result could potentially be that at 700 and 800 °C, the dominant active site changes from MoS₂ edges to another type. Based on the study by Li *et.al.* on all the catalytic sites of MoS₂ for HER, in addition to the well-known catalytically active edges, sulfur vacancies provide another major active sites for HER.⁵² The high-temperature H₂ annealing might have created local sulfur depletion of MoS₂, which is capable of catalyzing the HER. The exact mechanism of this phenomenon needs to be further studied and verified by detailed chemical compositional and structural information using characterization techniques such as X-ray photoelectron spectroscopy or high-resolution TEM.

The total electrode activity of untreated and H₂ etched samples are summarized in Fig. 6c. The 600 °C sample performs slightly better than the untreated one despite lower intrinsic activity because it can be compensated by the largely increased number of surface area and edge density. The samples under 700 and 800 °C conditions demonstrate significantly enhanced overall HER activity owing to

the increased surface area resulted larger number of active sites. 800 °C leads to a slightly lower overall HER activity than 700 °C because of the material loss and decomposition (as evidenced by the surface area measurement in Fig. 6a) under such high temperature and reducing gas agent.

Both surface area evaluation and electrochemical measurements demonstrate that 700 °C annealing results in the optimal real surface area enhancement and HER activity improvement (see Fig. 6b and c) with smallest Tafel slope (Fig. 6d) and largest exchange current density (Table 1). Optimum condition is a compromise between active site density increase and active material loss. EIS measurement in Fig. S4 confirms that the H₂ annealing doesn't change the conductivity of MoS₂ catalyst system ($\sim 20 \Omega/\text{cm}^2$). With the 800 °C sample, 2-regime Tafel slope is observed. It indicates that the sample undergoes a transition of rate-limiting step from the Heyrovsky to the Volmer reaction at the overpotential of ~ 300 mV vs. RHE, which may correspond to the switching of dominant type of the catalyzing active sites.

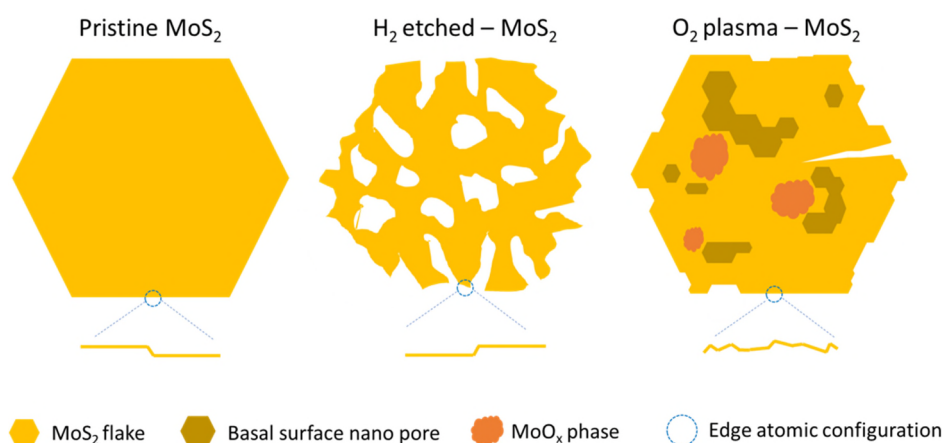


Figure 7. Schematic model of structural modification via defect engineering in MoS₂ nanoflakes: a comparison between O₂ plasma treatment and H₂ etching.

To summarize and compare the different defects introduced by two engineering methods used in this study, based on SEM and TEM analysis results as discussed in Fig. 2 and 5, the schematic model is shown in Fig. 7 to illustrate the single MoS₂ domain structure as of the as-grown, H₂ etched and O₂

plasma treated samples. Compared with pristine MoS₂, irregular network of nanoribbons and nanoholes are generated by H₂ annealing process onto the basal surfaces and edges. As to O₂ plasma treatment, roughened edges, microcracks, quasi-ordered chained surface damage as well as second phase – MoO_x are the main defect configuration.

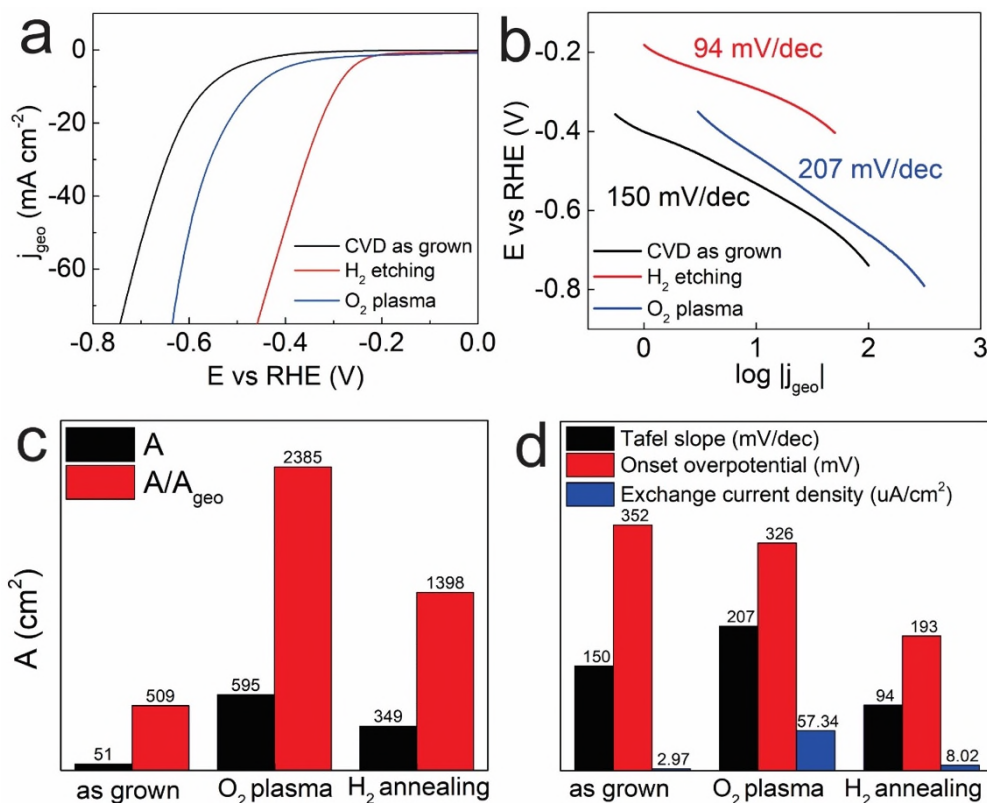


Figure 8. Comparison of real surface area enhancement and HER improvement for O₂ plasma treated and H₂ etched MoS₂ catalysts. (a) Cathodic polarization curves at scan rate of 1 mV/s, (b) Tafel plots, (c) surface area evaluation and (d) electrochemical metrics (Tafel slope, onset overpotential and exchange current density) of CVD as-grown, O₂ plasma and H₂ annealed samples.

The surface area enhancement is verified to be effective by both methods and can be easily controlled by tuning processing time and temperature; though the above mentioned structural difference leads to varied efficiency of the active sites density and HER improvement as illustrated in Fig. 8. O₂ plasma is twice as effective as H₂ annealing to increase surface area of the catalysts (A/A_{geo}: 2385 vs. 1398).

H₂ etching is better at enhancement of total HER activity as observed from the cathodic polarization curves (Fig. 8a and Table 1) that it lowers the onset overpotential by 159 mV. The enhancement attributes to creation of new type of active sites as well as increased surface area. On the other hand, the overall HER activity improvement by oxygen plasma relies mainly on the increased number of catalytic active edges.

Tafel slope value indicates the rate-limiting step of the pristine, O₂ plasma treated and H₂ etched samples is Volmer and Heyrovsky reaction. H₂ etching is more desirable for practical application since it facilitates enhanced current density (hydrogen generation per area) at a moderate increase of overpotential with the smallest Tafel slope in this study.

The as-optimized defect-rich MoS₂ catalysts exhibit promising HER electrocatalytic potential compared to other MoS₂ – only electrocatalysts from literature: 700 °C – H₂ – MoS₂ possesses Tafel slope of 94 mV/dec and low onset overpotential of 193 mV; 15 mins – O₂ – MoS₂ performs amongst the best with excellent exchange current density of 57 $\mu\text{A}/\text{cm}^2$ (normalized by geometric area).^{10,22,24,32,38,52,53} Detailed HER catalytic metrics comparison with literature can be found in Table 2. Especially compared with monolayer MoS₂ subject to similar process – CVD combined with O₂ plasma or H₂ etching, the defect engineered 3D-ER MoS₂ in this study exhibits j_{geo} (at $\eta=0.5$ mV) of 6-fold and 38-fold, for O₂ plasma and H₂ etching approaches respectively (Table 3), benefiting from maximized usage of electrode area by the unique 3D architecture.

In order to investigate the stability and durability of the defect-treated MoS₂ catalysts, ambient conditioned ageing combined with cycling treatment was conducted by exposing the as-prepared defect-rich samples to ambient air and light at room temperature for 2 years and then tested for HER post 1000 cycles to confirm stability. The HER activity of samples under optimum defect treatment conditions before and after ageing and cycling is summarised in Figure S5. The HER activity of O₂ plasma treated sample remained unchanged after ageing and cycles treatment. This confirms the

defects (additional edges and oxides) generated by O₂ plasma are adequately stable to endure the ambient air, temperature and light condition as well as long-term HER cycling. A certain degree of degradation in HER catalytic activity can be seen with the H₂ etched sample (Figure S5b), caused by the detachment of catalyst material from the electrode (Figure S5c-d). The detachment of catalyst from electrode is likely due to peeling-off effect of the generated gas bubbles at large current density. Future work needs to be conducted on enhancement of the adhesion between catalyst and glassy carbon electrode for intense HER catalysis at large current density range, by introducing adhesion layer between the catalyst and substrate layers or pre-treatment of substrate before deposition of MoS₂ catalyst.

Table 1. Electrocatalytic metrics towards HER for MoS₂ treated by O₂ plasma and H₂ annealing.

<i>Catalysts</i>		Onset overpotential (mV vs RHE)	Tafel slope (mV/dec)	Exchange current density ($\mu\text{A}/\text{cm}^2$)
<i>Pristine</i>		352	150	2.97
<i>Defect rich MoS₂ Catalysts</i>	<i>15 min O₂ Plasma Treated MoS₂</i>	326	207	57.34
	<i>30 min O₂ Plasma Treated MoS₂</i>	303	173	13.18
	<i>600 °C H₂ Etched MoS₂</i>	300	170	7.13
	<i>700 °C H₂ Etched MoS₂</i>	193	94	8.02
	<i>800 °C H₂ Etched MoS₂</i>	172	77 (200)	1.61

Table 2. Summary HER parameters of defect-rich MoS₂-only electrocatalysts from literature.

Catalyst	Media	Onset potential (mV vs RHE)	Tafel slope (mV/decade)	j ₀ -geometric (μA/cm ²)
Plasma-engineered MoS ₂ thin-film ³⁸	0.5M H ₂ SO ₄	-	105	-
Sulfur vacancy rich MoS ₂ monolayer thin film ⁵²	0.5M H ₂ SO ₄	-	65 – 85	40
Defect-rich MoS ₂ nanowall ¹⁰	0.5M H ₂ SO ₄	95	78	450
Defect-rich MoS ₂ ultrathin nanosheets ²²	0.5M H ₂ SO ₄	120	50	8.91
Defects engineered monolayer MoS ₂ ²⁴	0.5M H ₂ SO ₄	300	117	-
Monolayer MoS ₂ with strained sulfur vacancies ³²	-	~ 0	82	~ 50
<i>15 min O₂ plasma treated MoS₂ (this study)</i>	<i>0.5M H₂SO₄</i>	<i>326</i>	<i>207</i>	<i>57.34</i>
<i>700 °C H₂ etched MoS₂ (this study)</i>	<i>0.5M H₂SO₄</i>	<i>193</i>	<i>94</i>	<i>8.02</i>

Table 3. j (mA/cm²) @η=0.5 mV for defect engineered monolayer and 3D-ER MoS₂.

Approaches	Monolayer ²⁴	3D-ER (this study)
H ₂ etching	2.5	95
O ₂ plasma	2.5	15

Conclusion

The defect-rich vertically standing MoS₂ nanoplatelets were successfully fabricated via CVD and subsequent O₂ plasma or H₂ etching approach to be utilized as electrocatalyst towards water splitting. By systematically controlling the defect processing parameters - O₂ plasma exposure time or H₂ annealing temperature, tunable surface area and catalytic activity enhancement can be obtained.

Insights were gained into correlation between microstructure change and catalytic activity improvement as well as comparison of the two defect engineering methods. The surface area was significantly enlarged in both cases but via different microstructure architectures. O₂ plasma treatment introduced basal micro-cracks and local surface damage as well as promoted saw-toothed edge configuration; H₂ etching generated irregular shaped basal surface nanopores and nanostrips. Electrochemical evaluation revealed that compared with H₂ etching, O₂ plasma was more effective in surface area enhancement, but less powerful in improving HER catalytic activity, which is attributed to O₂ plasma induced less active MoO_x phase into the catalyst system. H₂ etching enhances the overall HER activity by creating new type of active sites as well as increased surface area. Such as-designed defect-rich structure significantly enhanced edge density over geometric area, together with porous structure and superaerophobic surface, it enables us to construct highly effective non-noble metal catalyst system, which maximizes physical area usage of electrodes. Such defect engineering routes can be incorporated into many more Pt-free catalyst systems other than MoS₂ for improved functionality as well. This will broaden the economic application of electrocatalytic water splitting for hydrogen generation. To facilitate intense HER catalysis application at large current density range, further research should be conducted on enhancing the adhesion between catalyst and glassy carbon electrode to avoid catalyst peeling.

Experimental Method

Preparation of Defect Engineered MoS₂ Catalyst. The synthesis of edge-exposed MoS₂ thin film was realized by chemical vapor deposition (CVD) method directly on glassy carbon substrates using 500 mg of molybdenum (VI) oxide (MoO₃) powder ($\geq 99.5\%$ Sigma-Aldrich) powder and 600 mg sulfur powder ($\geq 99.5\%$, Sigma-Aldrich). Two-furnace double-quartz tube system was employed to realize separate control of temperatures of MoO₃ and S. The reaction system was protected from oxygen by Ar gas. Sulfur vapor was carried by Ar gas from the upstream of the low-temperature tube for

reaction. The temperatures for S, MoO₃ and glassy carbon substrates were set at 180 °C, ~ 380 °C and 800 °C in order to achieve vertical standing morphology. Growth stage was set for 60 mins with 50 s.c.c.m. of Ar gas. The CVD as grown MoS₂ edge exposed thin film on glassy carbon was subject of H₂ annealing procedure at 600 ~ 800 °C for 2 h under H₂ flow (20% in argon, 50 s.c.c.m.). After annealing, the sample was naturally cooled down to room temperature under the protection of argon gas. The O₂ plasma etching process of as grown MoS₂ was carried out at pressure of 0.8~1 mPa for 0 ~ 30 mins.

Characterization. Morphology and microstructure were analyzed by scanning electron microscopy (SEM), (aberration-corrected) transmission electron microscope ((AC-)TEM, respectively. SEM characterization was carried out on Hitachi S-4300 with an accelerating voltage of 3.0 kV. TEM samples were prepared by gently rubbing the TEM grid across the surface of the MoS₂ thin film to mechanical exfoliate flakes and promote their adhesion to the lacey carbon TEM grid. Low magnification TEM was performed using a JEOL JEM-2100 with an accelerating voltage of 200 kV and AC-TEM was performed using Oxford's JEOL JEM-2200MCO FEGTEM with a CEOS image corrector and operated at an accelerating voltage of 80 kV. Raman spectroscopy was measured using a JY Horiba Labram Aramis imaging con-focal Raman microscope with excitation wavelength of 532 nm.

Surface Area Evaluation. Based on Cottrell's equation, given homogeneous current distribution, the current, which is associated with the diffusion-controlled charge transfer to a reactant, is given by $i = nFADc/\delta$, where D is the diffusion coefficient, c the bulk concentration and δ the thickness of the diffusion layer. Under the proviso that $c = c$ at $t = 0$ and $c = 0$ at the electrode surface at $t > 0$, δ at time t is given by $\delta = \sqrt{(\pi Dt)}$. Then by potentiostatically recording the current as a function of time: $A = i/nFc/\sqrt{(D/\pi t)}$, the surface area of the catalyst can be determined via the reaction of K₃Fe(CN)₆ → K₄Fe(CN)₆. Geometric area of the samples in this study is 0.1 or 0.25 cm².

Electrochemical Testing. A three-electrode setup was used for measurement of electrocatalytic activities towards HER in 0.5 M H₂SO₄ Ar-purged solution. Ag/AgCl/KCl (3M) (E (RHE) = E (Ag/AgCl / KCl (3M)) + 0.21 – 0.059·pH), activated carbon and 1 mm thick glassy carbon plate (Sigma-Aldrich Company Ltd) containing defect-engineered MoS₂ films were employed as reference, counter and working electrode, respectively. The effective area (0.5 cm × 0.5 cm) of the working electrode was defined by electrochemically inert pure polytetrafluoroethylene (PTFE) tape. A metal clip was used to connect the working electrode with an external circuit. Linear sweep voltammetry (*abbrev.* LSV, scan rate of 1 mV/s) under quasi-equilibrium conditions were performed by a Biologic VMP3 potentiostat. The Electrochemical Impedance Spectroscopy (*abbrev.* EIS) was carried out from 200000 to 1 Hz with an perturbation amplitude of 10 mV.

References

- (1) Xu, W.; Fang, Q.; Liu, D.; Zhang, K.; Habib, M.; Wu, C.; Zheng, X.; Liu, H.; Chen, S.; Song, L. Growing and Etching MoS₂ on Carbon Nanotube Film for Enhanced Electrochemical Performance. *Molecules* 2016, 21, 1–10.
- (2) Vrubel, H.; Moehl, T.; Grätzel, M.; Hu, X. Revealing and Accelerating Slow Electron Transport in Amorphous Molybdenum Sulphide Particles for Hydrogen Evolution Reaction. *Chem. Commun.* 2013, 49, 8985–8987.
- (3) Laursen, A. B.; Vesborg, P. C. K.; Chorkendorff, I. A High-Porosity Carbon Molybdenum Sulphide Composite with Enhanced Electrochemical Hydrogen Evolution and Stability. *Chem. Commun.* 2013, 49, 4965–4967.
- (4) Ohi, J. Hydrogen Energy Cycle: An Overview. *J. Mater. Res.* 2005, 20, 3180–3187.
- (5) Chen, Z.; Cummins, D.; Reinecke, B. N.; Clark, E.; Sunkara, M. K.; Jaramillo, T. F. Core-Shell MoO₃-MoS₂ Nanowires for Hydrogen Evolution: A Functional Design for Electrocatalytic

Materials. Nano Lett. 2011, 11, 4168–4175.

(6) Morales-Guio, C. G.; Stern, L.-A.; Hu, X. Nanostructured Hydrotreating Catalysts for Electrochemical Hydrogen Evolution. Chem. Soc. Rev. 2014, 43, 6555–6569.

(7) Benck, J. D.; Hellstern, T. R.; Kibsgaard, J.; Chakthranont, P.; Jaramillo, T. F. Catalyzing the Hydrogen Evolution Reaction (HER) with Molybdenum Sulfide Nanomaterials. ACS Catal. 2014, 4, 3957–3971.

(8) Lu, Z.; Zhang, H.; Zhu, W.; Yu, X.; Kuang, Y.; Chang, Z.; Lei, X.; Sun, X. In Situ Fabrication of Porous MoS₂ Thin-Films as High-Performance Catalysts for Electrochemical Hydrogen Evolution. Chem. Commun. (Camb). 2013, 49, 7516–7518.

(9) Xu, W.; Li, S.; Zhou, S.; Lee, J. K.; Wang, S.; Sarwat, S. G.; Wang, X.; Bhaskaran, H.; Pasta, M.; Warner, J. H. Large Dendritic Monolayer MoS₂ Grown by Atmospheric Pressure Chemical Vapor Deposition for Electrocatalysis. ACS Appl. Mater. Interfaces 2018, 10, 4630–4639.

(10) Xie, J.; Qu, H.; Xin, J.; Zhang, X.; Cui, G.; Zhang, X.; Bao, J.; Tang, B.; Xie, Y. Defect-Rich MoS₂ Nanowall Catalyst for Efficient Hydrogen Evolution Reaction. Nano Res. 2017, 10, 1178–1188.

(11) Jaramillo, T. F.; Jørgensen, K. P.; Bonde, J.; Nielsen, J. H.; Horch, S.; Chorkendorff, I. Identification of Active Edge Sites for Electrochemical H₂ Evolution from MoS₂ Nanocatalysts. Science 2007, 317, 100–102.

(12) Zhang, X.; Zhang, S.; Chen, B.; Wang, H.; Wu, K.; Chen, Y.; Fan, J.; Qi, S.; Cui, X.; Zhang, L.; et al. Direct Synthesis of Large-Scale Hierarchical MoS₂ Films Nanostructured with Orthogonally Oriented Vertically and Horizontally Aligned Layers. Nanoscale 2016, 8, 431–439.

(13) Wang, H.; Zhang, Q.; Yao, H.; Liang, Z.; Lee, H. W.; Hsu, P. C.; Zheng, G.; Cui, Y. High

Electrochemical Selectivity of Edge versus Terrace Sites in Two-Dimensional Layered MoS₂ Materials. *Nano Lett.* 2014, 14, 7138–7144.

(14) Zhang, X. H.; Li, N.; Wu, J.; Zheng, Y. Z.; Tao, X. Defect-Rich O-Incorporated 1T-MoS₂ Nanosheets for Remarkably Enhanced Visible-Light Photocatalytic H₂ Evolution over CdS: The Impact of Enriched Defects. *Appl. Catal. B Environ.* 2018, 229, 227–236.

(15) Wang, H.; Lu, Z.; Xu, S.; Kong, D.; Cha, J. J.; Zheng, G.; Hsu, P. C.; Yan, K.; Bradshaw, D.; Prinz, F. B.; et al. Electrochemical Tuning of Vertically Aligned MoS₂ Nanofilms and Its Application in Improving Hydrogen Evolution Reaction. *Proc. Natl. Acad. Sci. U. S. A.* 2013, 110, 19701–19706.

(16) Behranginia, A.; Asadi, M.; Liu, C.; Yasaei, P.; Kumar, B.; Phillips, P.; Foroozan, T.; Waranius, J. C.; Kim, K.; Abiade, J.; et al. Highly Efficient Hydrogen Evolution Reaction Using Crystalline Layered Three-Dimensional Molybdenum Disulfides Grown on Graphene Film. *Chem. Mater.* 2016, 28, 549–555.

(17) Merki, D.; Fierro, S.; Vrubel, H.; Hu, X. Amorphous Molybdenum Sulfide Films as Catalysts for Electrochemical Hydrogen Production in Water. *Chem. Sci.* 2011, 2, 1262–1267.

(18) Jian, C.; Cai, Q.; Hong, W.; Li, J.; Liu, W. Enhanced Hydrogen Evolution Reaction of MoO_x/Mo Cathode by Loading Small Amount of Pt Nanoparticles in Alkaline Solution. *Int. J. Hydrogen Energy* 2017, 42, 17030–17037.

(19) Kong, D.; Wang, H.; Cha, J. J.; Pasta, M.; Koski, K. J.; Yao, J.; Cui, Y. Synthesis of MoS₂ and MoSe₂ Films with Vertically Aligned Layers. *Nano Lett.* 2013, 13, 1341–1347.

(20) Kibsgaard, J.; Chen, Z.; Reinecke, B. N.; Jaramillo, T. F. Engineering the Surface Structure of MoS₂ to Preferentially Expose Active Edge Sites for Electrocatalysis. *Nat. Mater.* 2012, 11, 963–

- (21) Wang, H.; Lu, Z.; Sun, J.; Hymel, T. M.; Cui, Y. Electrochemical Tuning of MoS₂ Nanoparticles on Three-Dimensional Substrate for Efficient Hydrogen. *ACS Nano* 2014, 8, 4940–4947.
- (22) Xie, J.; Zhang, H.; Li, S.; Wang, R.; Sun, X.; Zhou, M.; Zhou, J.; Lou, X. W.; Xie, Y. Defect-Rich MoS₂ Ultrathin Nanosheets with Additional Active Edge Sites for Enhanced Electrocatalytic Hydrogen Evolution. *Adv. Mater.* 2013, 25, 5807–5813.
- (23) Xie, J.; Zhang, J.; Li, S.; Grote, F.; Zhang, X.; Zhang, H.; Wang, R.; Lei, Y.; Pan, B.; Xie, Y. Controllable Disorder Engineering in Oxygen-Incorporated MoS₂ Ultrathin Nanosheets for Efficient Hydrogen Evolution. *J. Am. Chem. Soc.* 2013, 135, 17881–17888.
- (24) Ye, G.; Gong, Y.; Lin, J.; Li, B.; He, Y.; Pantelides, S. T.; Zhou, W.; Vajtai, R.; Ajayan, P. M. Defects Engineered Monolayer MoS₂ for Improved Hydrogen Evolution Reaction. *Nano Lett.* 2016, 16, 1097–1103.
- (25) Lu, Z.; Zhu, W.; Yu, X.; Zhang, H.; Li, Y.; Sun, X.; Wang, X.; Wang, H.; Wang, J.; Luo, J.; et al. Ultrahigh Hydrogen Evolution Performance of Under-Water “Superaerophobic” MoS₂ Nanostructured Electrodes. *Adv. Mater.* 2014, 26, 2683–2687.
- (26) Yang, Y.; Fei, H.; Ruan, G.; Xiang, C.; Tour, J. M. Edge-Oriented MoS₂ Nanoporous Films as Flexible Electrodes for Hydrogen Evolution Reactions and Supercapacitor Devices. *Adv. Mater.* 2014, 26, 8163–8168.
- (27) Kong, D.; Wang, H.; Cha, J. J.; Pasta, M.; Koski, K. J.; Yao, J.; Cui, Y. Synthesis of MoS₂ and MoSe₂ Films with Vertically Aligned Layers. *Nano Lett.* 2013, 13, 1341–1347.
- (28) Li, S.; Wang, S.; Salamone, M. M.; Robertson, A. W.; Nayak, S.; Kim, H.; Tsang, S. E.;

Pasta, M.; Warner, J. H. Edge Enriched 2D MoS₂ Thin Films Grown by Chemical Vapor Deposition for Enhanced Catalytic Performance. *ACS Catal.* 2017, 7, 877–886.

(29) Hou, Y.; Zhang, B.; Wen, Z.; Cui, S.; Guo, X.; He, Z.; Chen, J. A 3D Hybrid of Layered MoS₂/Nitrogen-Doped Graphene Nanosheet Aerogels: An Effective Catalyst for Hydrogen Evolution in Microbial Electrolysis Cells. *J. Mater. Chem. A* 2014, 2, 13795–13800.

(30) Li, B.; Cheng, Z.; Zhang, N.; Sun, K. Self-Supported, Binder-Free 3D Hierarchical Iron Fluoride Flower-like Array as High Power Cathode Material for Lithium Batteries. *Nano Energy* 2014, 4, 7–13.

(31) Hai, X.; Zhou, W.; Wang, S.; Pang, H.; Chang, K.; Ichihara, F.; Ye, J. Rational Design of Freestanding MoS₂ Monolayers for Hydrogen Evolution Reaction. *Nano Energy* 2017, 39, 409–417.

(32) Li, H.; Tsai, C.; Koh, A. L.; Cai, L.; Contryman, A. W.; Fragapane, A. H.; Zhao, J.; Han, H. S.; Manoharan, H. C.; Abild-Pedersen, F.; et al. Activating and Optimizing MoS₂ Basal Planes for Hydrogen Evolution through the Formation of Strained Sulphur Vacancies. *Nat. Mater.* 2015, 15, 48–53.

(33) Zhang, X. H.; Li, N.; Wu, J.; Zheng, Y. Z.; Tao, X. Defect-Rich O-Incorporated 1T-MoS₂ Nanosheets for Remarkably Enhanced Visible-Light Photocatalytic H₂ Evolution over CdS: The Impact of Enriched Defects. *Appl. Catal. B Environ.* 2018, 229, 227–236.

(34) Krivosheeva, A. V.; Shaposhnikov, V. L.; Borisenko, V. E.; Lazzari, J.-L.; Waileong, C.; Gusakova, J.; Tay, B. K. Theoretical Study of Defect Impact on Two-Dimensional MoS₂. *J. Semicond.* 2015, 36, 122002.

(35) Spirko, J. A.; Neiman, M. L.; Oelker, A. M.; Klier, K. Electronic Structure and Reactivity of Defect MoS₂: I. Relative Stabilities of Clusters and Edges, and Electronic Surface States. *Surf. Sci.*

2003, 542, 192–204.

(36) Zhou, W.; Zou, X.; Najmaei, S.; Liu, Z.; Shi, Y.; Kong, J.; Lou, J.; Ajayan, P. M.; Yakobson, B. I.; Idrobo, J. C. Intrinsic Structural Defects in Monolayer Molybdenum Disulfide. *Nano Lett.* 2013, 13, 2615–2622.

(37) Yang, L.; Zhou, W.; Lu, J.; Hou, D.; Ke, Y.; Li, G.; Tang, Z.; Kang, X.; Chen, S. Hierarchical Spheres Constructed by Defect-Rich MoS₂/Carbon Nanosheets for Efficient Electrocatalytic Hydrogen Evolution. *Nano Energy* 2016, 22, 490–498.

(38) Tao, L.; Duan, X.; Wang, C.; Duan, X.; Wang, S. Plasma-Engineered MoS₂ Thin-Film as an Efficient Electrocatalyst for Hydrogen Evolution Reaction. *Chem. Commun. (Camb)*. 2015, 51, 7470–7473.

(39) Wei, X.; Yu, Z.; Hu, F.; Cheng, Y.; Yu, L.; Wang, X.; Xiao, M.; Wang, J.; Wang, X.; Shi, Y. Mo-O Bond Doping and Related-Defect Assisted Enhancement of Photoluminescence in Monolayer MoS₂. *AIP Adv.* 2014, 4, 123004.

(40) Xiao, S.; Xiao, P.; Zhang, X.; Yan, D.; Gu, X.; Qin, F.; Ni, Z.; Han, Z. J.; Ostrikov, K. Atomic-Layer Soft Plasma Etching of MoS₂. *Sci. Rep.* 2016, 6, 19945.

(41) Kang, N.; Paudel, H. P.; Leuenberger, M. N.; Tetard, L.; Khondaker, S. I. Photoluminescence Quenching in Single-Layer MoS₂ via Oxygen Plasma Treatment. *J. Phys. Chem. C* 2014, 118, 21258–21263.

(42) Takeno, T.; Abe, S.; Adachi, K.; Miki, H.; Takagi, T. Deposition and Structural Analyses of Molybdenum-Disulfide (MoS₂)-Amorphous Hydrogenated Carbon (a-C:H) Composite Coatings. *Diam. Relat. Mater.* 2010, 19, 548–552.

(43) Ionescu, R.; George, A.; Ruiz, I.; Favors, Z.; Mutlu, Z.; Liu, C.; Ahmed, K.; Wu, R.; Jeong, J.

- S.; Zavala, L.; et al. Oxygen Etching of Thick MoS₂ Films. *Chem. Commun.* 2014, 50, 11226–11229.
- (44) Geng, D.; Wu, B.; Guo, Y.; Luo, B.; Xue, Y.; Chen, J.; Yu, G.; Liu, Y. Fractal Etching of Graphene. *J. Am. Chem. Soc.* 2013, 135, 6431–6434.
- (45) Zhang, Y.; Li, Z.; Kim, P.; Zhang, L.; Zhou, C. Anisotropic Hydrogen Etching of Chemical Vapor Deposited Graphene. *ACS Nano* 2012, 6, 126–132.
- (46) Mouri, S.; Miyauchi, Y.; Matsuda, K. Tunable Photoluminescence of Monolayer MoS₂ via Chemical Doping. *Nano Lett.* 2013, 13, 5944–5948.
- (47) Wu, Z.; Fang, B.; Wang, Z.; Wang, C.; Liu, Z.; Liu, F.; Wang, W.; Alfantazi, A.; Wang, D.; Wilkinson, D. P. MoS₂ Nanosheets: A Designed Structure with High Active Site Density for the Hydrogen Evolution Reaction. *ACS Catal.* 2013, 3, 2101–2107.
- (48) Wang, S.; Wang, X.; Warner, J. H. All Chemical Vapor Deposition Growth of MoS₂:h-BN Vertical van Der Waals Heterostructures. *ACS Nano* 2015, 9, 5246–5254.
- (49) Yan, Y.; Xia, B.; Xu, Z.; Wang, X. Recent Development of Molybdenum Sulfides as Advanced Electrocatalysts for Hydrogen Evolution Reaction. *ACS Catal.* 2014, 4, 1693–1705.
- (50) Vrubel, H.; Merki, D.; Hu, X. Hydrogen Evolution Catalyzed by MoS₃ and MoS₂ Particles. *Energy Environ. Sci.* 2012, 5, 6136–6144.
- (51) Chang, Y. H.; Lin, C. T.; Chen, T. Y.; Hsu, C. L.; Lee, Y. H.; Zhang, W.; Wei, K. H.; Li, L. J. Highly Efficient Electrocatalytic Hydrogen Production by MoS_x Grown on Graphene-Protected 3D Ni Foams. *Adv. Mater.* 2013, 25, 756–760.
- (52) Li, G.; Zhang, D.; Qiao, Q.; Yu, Y.; Peterson, D.; Zafar, A.; Kumar, R.; Curtarolo, S.; Hunte, F.; Shannon, S.; et al. All The Catalytic Active Sites of MoS₂ for Hydrogen Evolution. *J. Am. Chem.*

Soc. 2016, 138, 16632–16638.

(53) Gao, M.-R.; Chan, M. K. Y.; Sun, Y. Edge-Terminated Molybdenum Disulfide with a 9.4-Å Interlayer Spacing for Electrochemical Hydrogen Production. *Nat. Commun.* 2015, 6, 7493.

(54) Cao, H.; Xiao Y.; Lu Y.; Yin J.; Li B.; Wu S.; Wu X. Ag₂Se Complex Nanostructures with Photocatalytic Activity and Superhydrophobicity. *Nano Res.* 2010, 3, 863-873.

(55) Xiao Y.; Cao, H.; Liu K.; Zhang S.; Chernow V. The synthesis of superhydrophobic Bi₂S₃ complex nanostructures. *Nanotechnology* 2010, 21, 145601.

Supporting Information

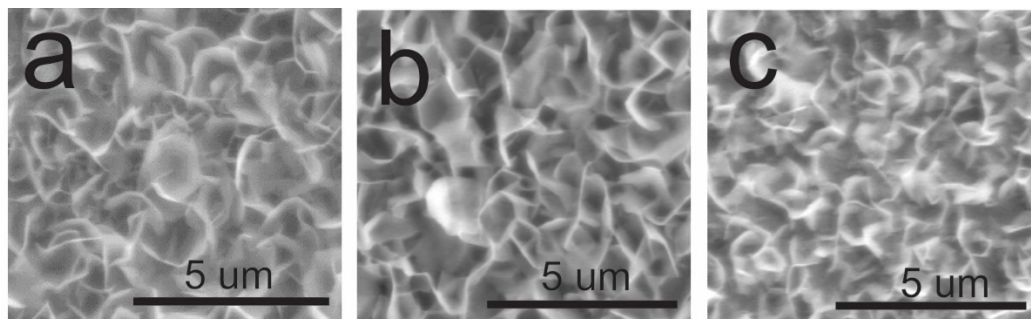


Figure. S1 SEM images depicting morphology evolution of MoS₂ thin films etched by O₂ plasma for (a) 0, (b) 15 and (c) 30 mins respectively.

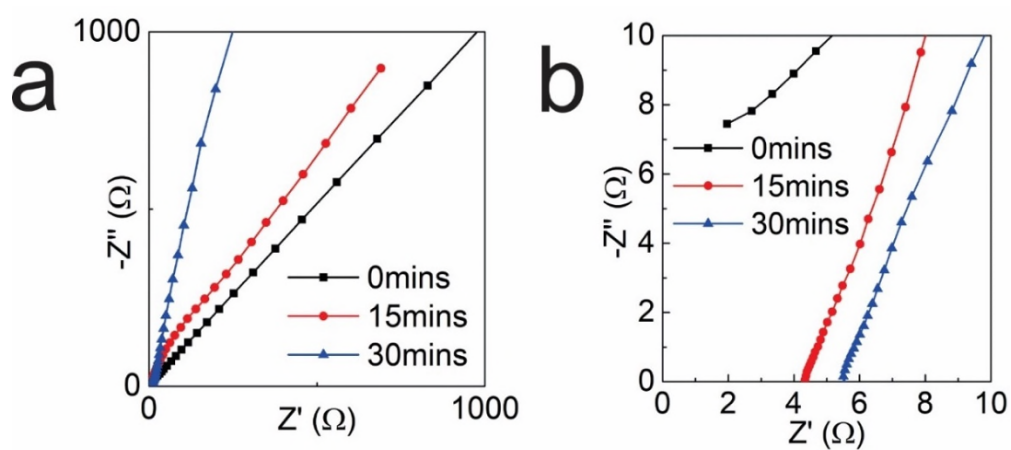


Figure. S2 Electrochemical impedance spectroscopy (EIS) of O₂-plasma etched MoS₂ catalysts as a function of plasma exposure time.

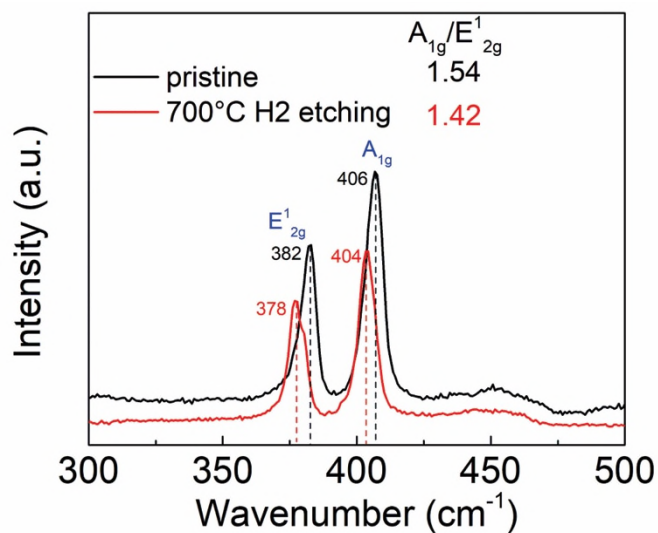


Figure. S3 Raman spectra of pristine and 700 °C H₂ etched MoS₂ catalysts. Inset: two characteristic Raman vibration modes in MoS₂: in-plane vibration of molybdenum and sulfur atoms E_{2g}¹ and out-of-plane vibration of sulfur atoms A_{1g}; information on peak intensity ratio of A_{1g}/E_{2g}¹ of samples before and after H₂ etching.

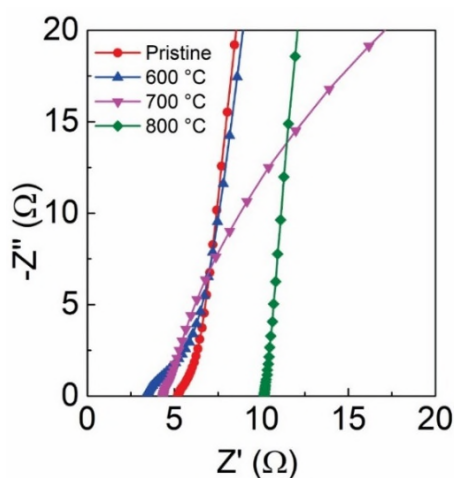


Figure. S4 Electrochemical impedance spectroscopy (EIS) of H₂-etched MoS₂ catalysts under different temperatures.

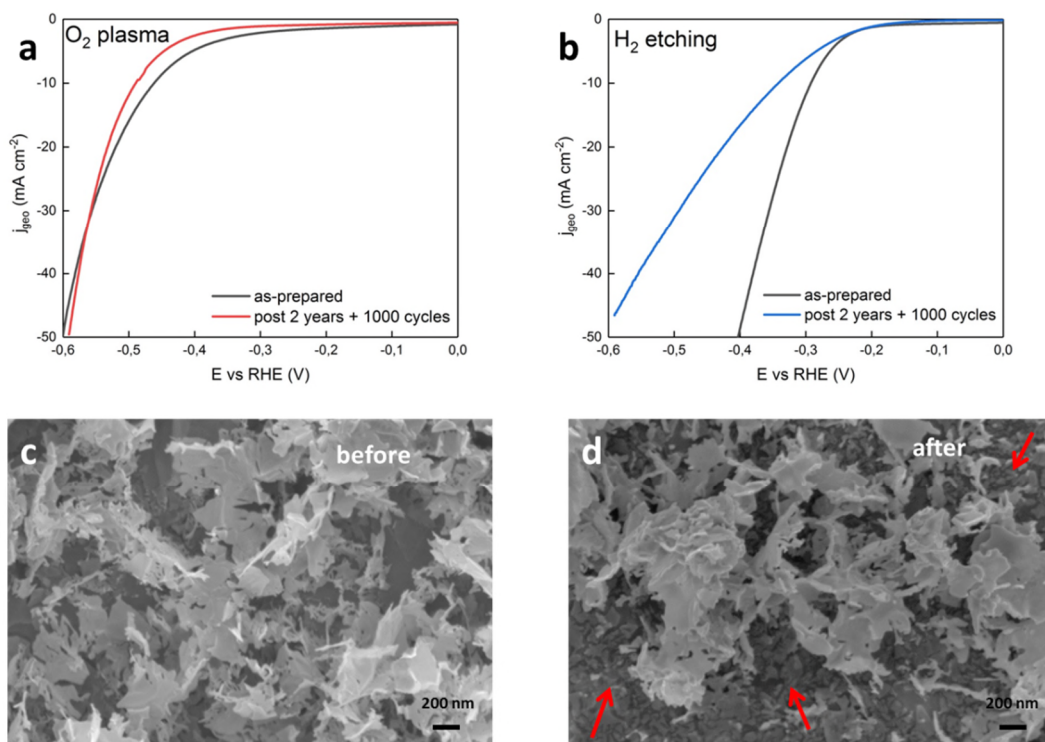


Figure. S5 HER stability of the defect-treated MoS_2 catalysts. HER activity of (a) O_2 plasma treated and (b) H_2 etched samples before and after ageing and cycling. SEM images of H_2 etched sample (c) before and (d) after cycling treatment.

In order to investigate the stability and durability of the defect-treated MoS_2 catalysts, ambient conditioned ageing combined with cycling treatment was conducted by exposing the as-prepared defect-rich samples to ambient air and light at room temperature for 2 years and then tested for HER post 1000 cycles to confirm stability.

The HER activity of samples under optimum defect treatment conditions before and after ageing and cycling is summarised in **Figure S5**. As shown in Figure S5a, the HER activity of O_2 plasma treated sample remained unchanged after 2-year-ageing and 1000 cycles treatment. This confirms the defects (additional edges and oxides) generated by O_2 plasma are adequately stable to endure the ambient air, temperature and light condition as well as long-term HER cycling.

A certain degree of degradation in HER catalytic activity can be seen with the H₂ etched sample (Figure S5b), caused by the detachment of catalyst material from the electrode (as seen from the SEM images before and after cycling treatment in Figure S5c-d, with red arrows indicating catalyst peeled-off areas). The detachment of catalyst from electrode is likely due to peeling-off effect of the generated gas bubbles at large current density. As H₂ etched sample is much more HER active than the O₂ plasma treated sample, much larger amount of gas bubbles are generated during the intense catalysis process and this leads to heavier peeling-off of catalyst from substrate.

To enhance the adhesion between catalyst and glassy carbon electrode for intense HER catalysis at large current density range, possible approaches include introducing an extra adhesion layer between the catalyst and substrate layers or surface pre-treatment of substrate before deposition of MoS₂ catalyst. This will follow in our future research work.

Table S1. Plasma treatment recipes for different MoS₂ materials from literature.

Material	Power/W	Pressure			Time/s	Gas
		mbar	Pa	Torr		
Thin film ¹	100	0.4	40	0.3	0-720	Oxygen/Argon
Monolayer ²	100	0.4	40	0.25-0.35	0-6	Oxygen 30%, argon 80%
Monolayer ³	100	0.33	33	0.25	0-6	Oxygen 30%, argon 80%
Monolayer ⁴	25	0.26	26	0.2	5	Argon
Monolayer ⁵	300	13.33	1333	10	0-30	Oxygen
Few layer (20 nm) ⁶	30-50	0.007	0.7	-	300	Nitrogen

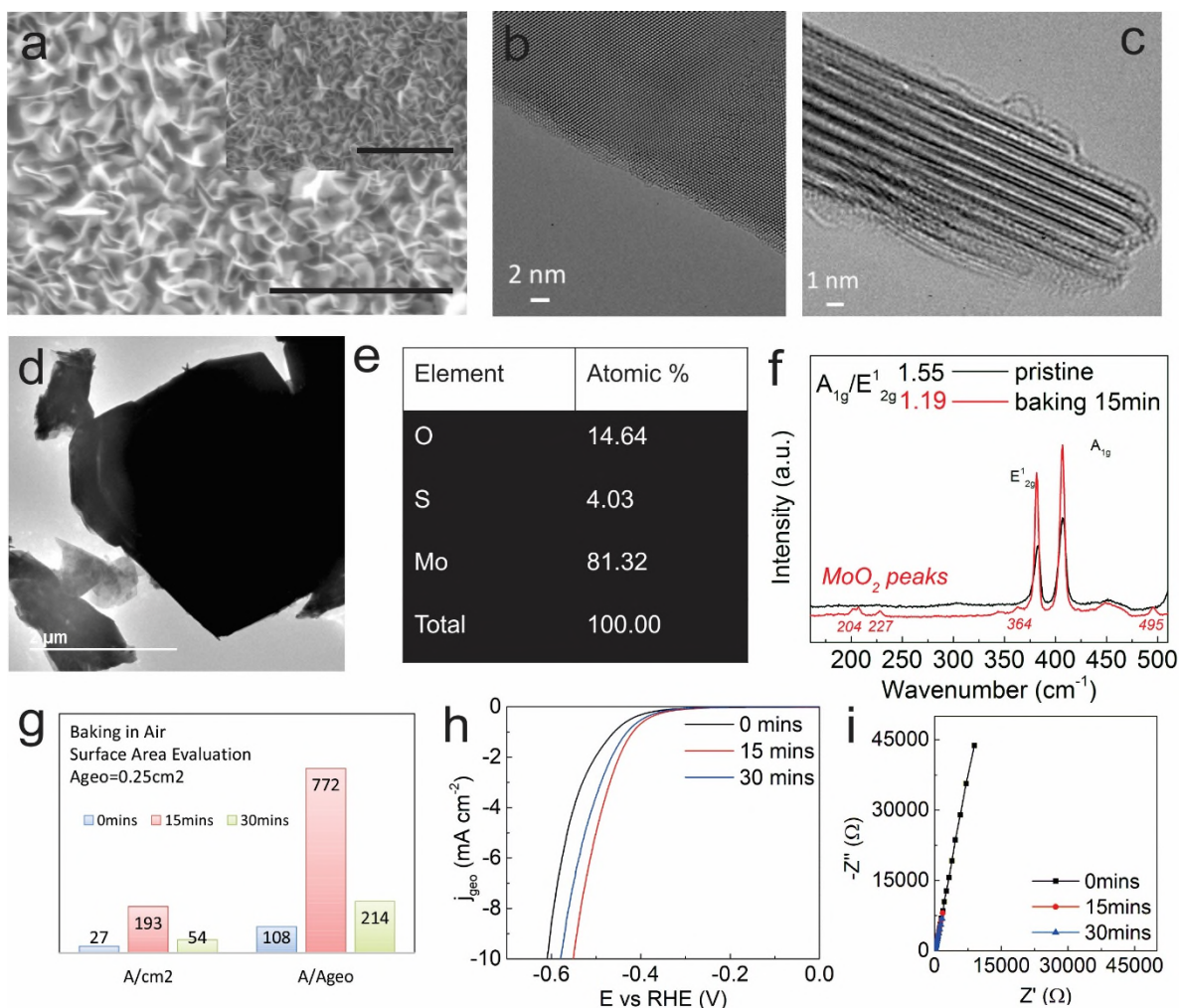


Figure S6. Influence of ambient air condition baking time on morphology, structure, chemical and HER activity of MoS₂ nanoplatelets. (a-c) SEM and HRTEM images of the 15 min baked sample, inset is SEM image of CVD as grown pristine MoS₂. (d and e) TEM image and energy dispersive X-ray analysis (EDX) determined elemental composition of MoO_x/MoS₂ composite. (f) Raman spectra of pristine and 15 mins baked MoS₂ catalysts. Inset: two characteristic Raman vibration modes in MoS₂: in-plane vibration of molybdenum and sulfur atoms E_{12g}¹ and out-of-plane vibration of sulfur atoms A_{1g}; information on peak intensity ratio of A_{1g}/E_{12g}¹ of samples before and after ambient air baking treatment; oxidation induced peaks. (g) Surface area evaluation as a function of baking time (A_{geo}: geometric area of the catalyst; A: real surface area of the catalyst). (h) Cathodic polarization curves at scan rate of 1 mV/s (insets: corresponding Tafel slopes and exchange current densities) and

(i) electrochemical impedance spectroscopy (EIS) of nanoplateleted MoS₂ catalysts as a function of baking time.

Baking was realized by placing the samples on hot plate at 300 °C for 0 – 30 mins. SEM images and electrochemistry testing were conducted before and after the treatment. Basically, there is no obvious change in platelet size change from SEM. The 15 mins baked sample was observed under the HRTEM, nice and clean vertical flake and zigzag edges can be seen. Also MoO_x/MoS₂ was detected under TEM and further confirmed by EDX elemental composition analysis. HER activity is increased mainly from lowered impedance of the samples and increased surface area. Tafel slope is slightly improved. 15 min ambient air baking is the most effective by comparing surface area, Tafel slopes and exchange current densities.

References

- (1) Tao, L.; Duan, X.; Wang, C.; Duan, X.; Wang, S. Plasma-Engineered MoS₂ Thin-Film as an Efficient Electrocatalyst for Hydrogen Evolution Reaction. *Chem. Commun. (Camb)*. 2015, 51, 7470–7473.
- (2) Islam, M. R.; Kang, N.; Bhanu, U.; Paudel, H. P.; Erementchouk, M.; Tetard, L.; Leuenberger, M. N.; Khondaker, S. I. Tuning the Electrical Property via Defect Engineering of Single Layer MoS₂ by Oxygen Plasma. *Nanoscale* 2014, 6, 10033.
- (3) Kang, N.; Paudel, H. P.; Leuenberger, M. N.; Tetard, L.; Khondaker, S. I. Photoluminescence Quenching in Single-Layer MoS₂ via Oxygen Plasma Treatment. *J. Phys. Chem. C* 2014, 118, 21258–21263.
- (4) Chow, P. K.; Jacobs-Gedrim, R. B.; Gao, J.; Lu, T. M.; Yu, B.; Terrones, H.; Koratkar, N. Defect-Induced Photoluminescence in Monolayer Semiconducting Transition Metal Dichalcogenides. *ACS Nano* 2015, 9, 1520–1527.

- (5) Ye, G.; Gong, Y.; Lin, J.; Li, B.; He, Y.; Pantelides, S. T.; Zhou, W.; Vajtai, R.; Ajayan, P. M. Defects Engineered Monolayer MoS₂ for Improved Hydrogen Evolution Reaction. *Nano Lett.* 2016, 16, 1097–1103.
- (6) Su, T.-H.; Lin, Y.-J. Effects of Nitrogen Plasma Treatment on the Electrical Property and Band Structure of Few-Layer MoS₂. *Appl. Phys. Lett.* 2016, 108, 033103.